Coordination Chemistry Reviews 254 (2010) 297–308

Contents lists available at ScienceDirect

Coordination Chemistry Reviews

journal homepage: www.elsevier.com/locate/ccr

Review

Application of low-temperature rapid-scan techniques in the elucidation of inorganic reaction mechanisms

Rudi van Eldik*, Colin D. Hubbard

Department of Chemistry and Pharmacy, University of Erlangen-Nürnberg, Egerlandstrasse 1, 91058 Erlangen, Germany

Contents

ARTICLE INFO

Article history:
Received 30 June 2009
Accepted 6 September 2009
Available online 11 September 2009

Keywords:
Low-temperature rapid scan
Activation of small molecules
Inorganic reaction mechanisms

ABSTRACT

Reactions that occur too rapidly to be monitored by rapid reaction methods at temperatures at or close to ambient can be investigated kinetically by retarding their reaction rates employing very low temperatures. A selection of reactions studied by this approach (low-temperature stopped-flow spectrophotometry) is reported. Details of the reaction mechanisms have been revealed for peroxide activation involving iron(III) porphyrins and cytochrome P450, superoxide activation involving manganese(II) complexes and iron porphyrin complexes, and dioxygen activation and binding by model mono-, and dinuclear copper(I) complexes and dioxygen activation at mono-, and dinuclear non-heme iron complexes. A final section covers progress in unravelling the mechanism of carbon–hydrogen bond activation by platinum complexes.

1. Introduction

The three editions of "Kinetics and Mechanism", the first two editions by A.A. Frost and R.G. Pearson, and the third by J.W. Moore and R.G. Pearson, will be well known to countless students and research investigators, particularly during the period 1950–1990 [1]. Furthermore two editions of "Mechanisms of Inorganic Reactions", authored by F. Basolo and R.G. Pearson, established a foundation for the blossoming subject, particularly for solution reactions [2]. Both landmark publications, in later editions, were able to account for the growth of development of fast reaction methods that allowed a whole new time window of reaction rates that could be studied [3–5]. Not content to rest with these successes, Professor Ralph Pearson is a principal proponent of the hard and soft acids and bases (HSAB) concept [6]. Recently he has authored an article seeking to link chemical hardness with density

* Corresponding author.
E-mail address: vaneldik@chemie.uni-erlangen.de (R. van Eldik).

0010-8545/$ – see front matter © 2009 Elsevier B.V. All rights reserved.
doi:10.1016/j.ccr.2009.09.009

functional theory [7]. It is important that pioneers in chemistry are recognized and acknowledged for their contributions. Therefore, the authors pay tribute to Ralph Pearson both for the cited works and countless additional research publications he has authored or coauthored in more than 60 years. In this article kinetics and mechanism are featured.

2. Experimental considerations: transient state species, pre-steady state species, rapidly reacting intermediates

In some chemical reactions, in order to generate a complete description from reactant state to the product state, from a kineticist's point of view, establishing the rate-determining step is only one objective and detecting and characterizing any intermediates or transient species are vital. In this way determination of the overall reaction mechanism may be more realizable. An investigator may require methods and techniques for following a reaction that is rapid overall (many proton transfer reactions involving an O–H or an N–H bond, for example), or for a reaction that is of conventional time range overall, yet has rapid steps within that overall time frame (many enzyme catalyzed reactions, for example). The range of techniques that can be employed to study rapid reactions, including flow methods, stopped-flow (sf), with or without quenching, relaxation methods (single perturbation, or oscillating field methods), NMR or ESR spectroscopies and photochemical methods, has been documented [3–5,8–11]. Examples of reactions studied in these pioneering reports are also cited. The basic principles of these experimental methods are largely unchanged, but now have better sensitivity, improved resolution, and data acquisition and data processing methods have been substantially modernised. Not every method is suitable for many reactions, as the time windows vary within fast reaction methods and compromises are needed, and individual properties of each reaction system need to be assessed before experimental design is initiated. Sometimes specifically designed instrumentation for a particular reaction series has been used, for example, a continuous flow method for ionic reactions monitored by conductivity changes [12]. In other cases indirect methods have been used to obtain kinetic characteristics of rapid reactions that cannot be monitored directly [13]. Another approach involved setting up a steady state by a constant rate of addition of a reactant, thus enabling a moderately fast reaction to be monitored [14].

Here, employment of temperatures not only below ambient, but also significantly below 0 °C is a focus. For reactions in the time range of a few minutes at ambient temperature, and where kinetic measurements are not comfortably made, reaction progress can be retarded either by diluting the reactant solutions or by lowering the temperature. However, with standard instruments involving exposed optical surfaces, condensation that increases with progressive lowering of temperature can cause a problem. In UV/vis spectrophotometric applications, designs involving fiber optics can circumvent this problem. When reactions under investigation are too rapid at temperatures near ambient for a standard stopped-flow method and are not suitable based upon their thermodynamic properties for study by a relaxation method (usually with faster capability), the reaction may be investigated by the sf method at lowered temperatures.

Interestingly part of the drive to develop this capability arose several decades ago [15]. It had been proposed that particular proton transfer reactions would occur not by the usual, accepted process of surmounting an energy barrier, but under certain conditions by the proton tunnelling through the energy barrier, based upon arguments from quantum mechanics [16]. The experimental criteria that would explain or validate the occurrence of tunnelling included among other properties, a value of a kinetic isotope effect

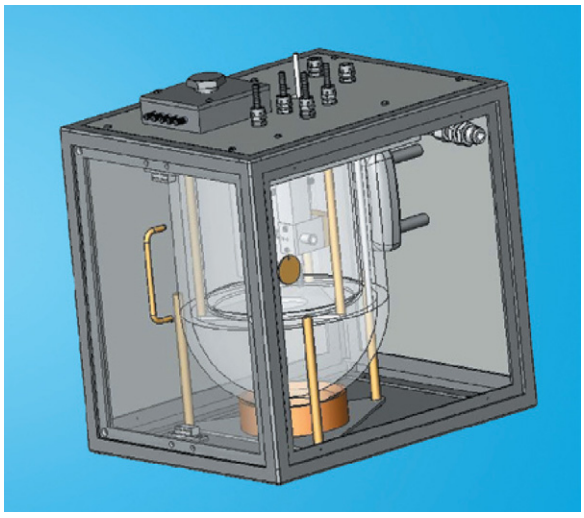

Fig. 1. Cryostat stopped-flow spectrophotometer. Figure supplied by TgK Scientific Ltd. [19].

(k_H/k_D) greater than 7 (at ambient temperature), but importantly for this topic, curvature of the Arrhenius plot for proton transfer, but not deuteron transfer, at *low temperatures*. Clearly, organic solvents were used, for example, in a series of experiments of reactions of aromatic nitro-compounds with bases over a range of 100 °C [15]. Compounds that were most amenable to study for potential detection of tunnelling were carbon acids (4-nitrophenylnitromethane, for example) in their reaction with bases such as amidines. Scrupulous drying of solvents was required and reactant design that avoided isotopic scrambling was critical. A review of the subject may be consulted [17]. A key feature of a low-temperature sf is that the cuvette/observation chamber is immersed in the cryostat fluid. Delivery of the reactant solutions to the mixing chamber and observation chamber is accomplished from syringes outside the cryostat. Likewise the stopping syringe and contents are outside the temperature bath. Fiber optics are used for incident radiation and detection of changes in UV/vis absorbance. Temperature control is often exercised by a double bath system of liquid nitrogen and low freezing solvent or it can be through use of cryostat fluid from an external separate bath. Early versions were laboratory/workshop built, and the design principles were adopted [18] and developed into commercially available apparatus (see Figs. 1 and 2). Resort to non-aqueous solvents may at times cause difficulties in relating mechanisms to those extant in *in vivo* reactions conditions.

An examination of the experimental section of many of the following publications reveal the technical challenges involved in studying reactions at low temperatures particularly when many of the reactants and products are water and/or air sensitive. In many cases it will be seen that molecular oxygen or anionic forms of oxygen in themselves are reagents. Therefore, the system must be designed to prevent incursion of adventitious oxygen; this means flow lines need to be comprised of materials that prevent diffusion through them of oxygen. Special features such as generating a reagent *in situ*, i.e. in a stopped-flow reactant syringe, or using a double mixing device are highlighted in some studies. However, each individual reacting system needs to be addressed based on its own characteristics, and it is not practicable to draw up a "one size fits all" experimental or methodological protocol.

3. Reaction mechanisms

This issue of Coordination Chemistry Reviews is concerned with Inorganic Reaction Mechanisms, a subject to which the authors

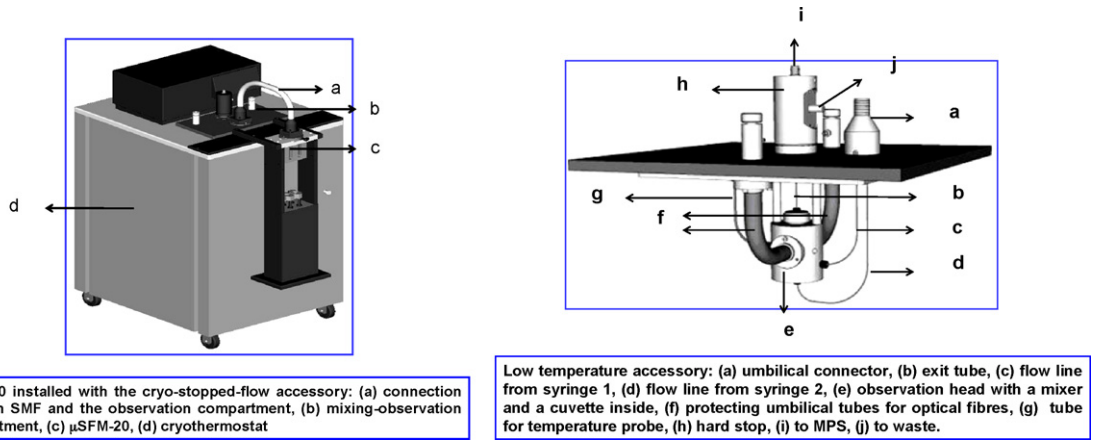

Fig. 2. Cryostat stopped-flow spectrophotometer.
Schematics supplied by Bio-Logic Science Instruments [20].

subscribe herein. In the selection of reaction systems whose mechanisms will be presented below, the liberty of extending this to bioinorganic reactions and to an organometallic reaction is exercised. The following sections are in no particular chronological order.

3.1. Peroxide activation

3.1.1. Cytochrome P450

Small molecules or ions such as nitric oxide, the superoxide ion and the peroxide ion have versatile biological functions; they can be involved in processes associated with oxidative stress, are implicated in defence mechanisms against micro-organisms and may serve as cellular signalling species [21]. NO and $O_2^{\bullet -}$ are radicals and react rapidly with each other, while H_2O_2 is a product of superoxide dismutase/reduction. Their roles are generally based on their redox activity and associated with transition metal centers. A principal aim has been to use a variety of techniques to study reaction steps of the activation of these species in order to contribute to a mechanistic understanding of the catalytic activity of various enzymes and related metal complexes. Relatively, the interaction of NO with cytochrome P450 or Fe(III) porphyrins and functional model complexes for P450 is straightforward involving a binding step and a charge transfer step, although variations in the rates and kinetic activation parameters and mechanisms are experienced at high and low pH values. These variations relate in part to a change in coordination number at the iron-center or different labilising affects in the axial position when a hydroxo ligand is present rather that a water molecule. The investigations leading to the generation of the kinetic and activation parameters for the interaction of NO with cytochrome P450 and related model compounds have been described [22–24].

The activation of peroxide involves coordination of peroxide to the Fe(III) center, followed by homolysis or heterolysis of the peroxo O–O bond, and formation of high oxidation state iron-oxo complexes that are able to transfer oxygen to inert substrate molecules.

3.1.2. Fe(III) porphyrins

The $Fe^{III}(TMPS^{4-})(H_2O)_2$ complex has a pK_a of 6.9, in aqueous solution, relating to the formation of the monohydroxo species, $Fe^{III}(TMPS^{4-})(OH^-)$, see Scheme 1.

In order to be able to monitor reactions with selected oxidants it became necessary to employ low temperatures (in the region of −30 to −40 °C), to be able to stabilize and characterize the oxidized porphyrin products formed at various pH values. A solvent mixture 4:1 (v/v) MeOH/H_2O, was employed as a cryosolvent, resulting in a change in the pK_a to 6.3 [25]. The axial positions of the complex could now be occupied by MeOH. The porphyrin complex was reacted with the peroxo-compound, *m*-chloroperoxybenzoic acid (*m*-CPBA), and followed using a low-temperature stopped-flow instrument. It prevailed that the nature of the products depended on the pH of study. At pH 5 a product was formed that showed an intense band in the Soret region and a broad absorbance band at higher wavelength, observations that indicated conversion to the oxoiron(IV) porphyrin cation radical $(TMPS^+)Fe^{IV}(O)$, a two electron oxidation process. At pH 9, in contrast, the product spectrum was analysed to indicate formation of $(TMPS)Fe^{IV}(O)$, from a one electron oxidation process. From the nature of the isosbestic points at both pH values, the reaction at −35 °C involves a single observable step. It was proposed, and supported by electrochemical experiments, and rapid-scan spectra that the variation of product with pH arises not from different legation at low and high pH but by a pH-tuned change in the redox properties of the complex. The spectra from which these conclusions were reached are presented in Fig. 3.

Upon varying the *m*-CPBA concentration, the observed first-order rate constants exhibited saturation at higher *m*-CPBA concentrations. This is usually a signal that the overall process consists of a rapid pre-equilibrium (in this case peroxide binding to the Fe(III) center) followed by a rate-determining step (cleavage of the O–O bond). The radical trap species ABTS (=diammonium-2,2′-alimonies(3-ethylbenzothiazoline-6-sulfonate)) can be used to trap the higher oxidation state oxo complexes by following the absorbance increase arising from the formation of the $ABTS^{\bullet +}$ radical cation. Mechanistic information could in principle be acquired from determination of the second-order rate constants for the catalyzed oxidation of ABTS by *m*-CPBA in the presence of $Fe(TMPS^{4-})$ as a function of temperature and pressure. Ideally all the reaction steps of the catalytic cycle in the scheme shown (see Scheme 2) would be thoroughly characterized.

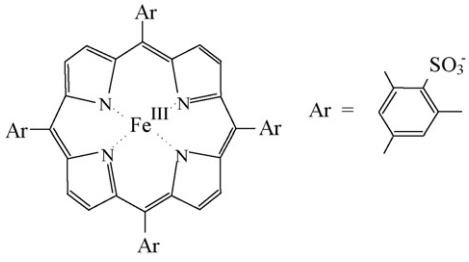

Scheme 1. Structure of $Fe^{III}(TMPS^{4-})$.

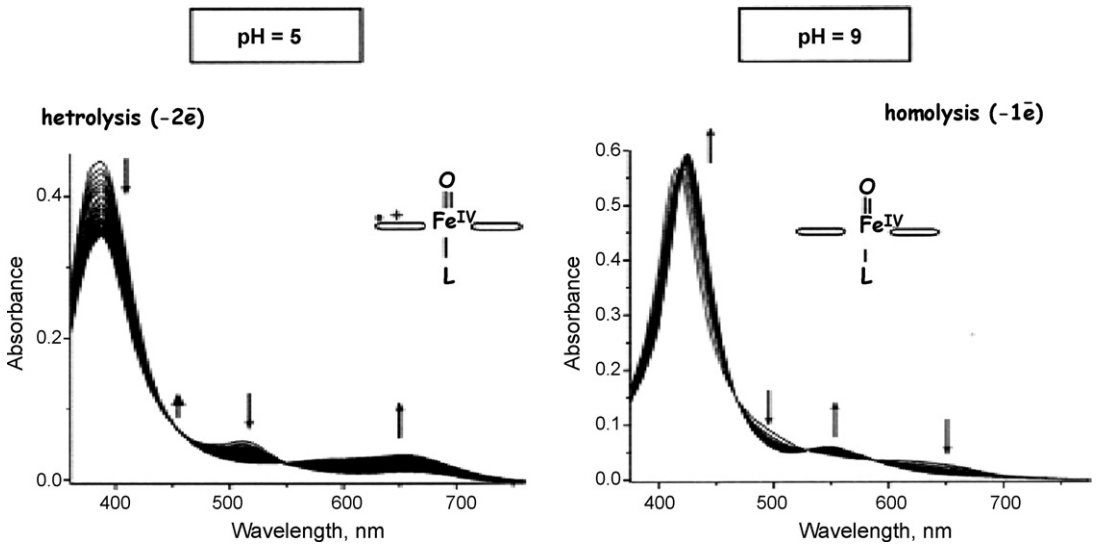

Fig. 3. Spectroscopic evidence for heterolytic and homolytic cleavage during the reaction of [$Fe^{III}(TMPS^{4-})$] with *m*-CPBA as a function of pH [21,25].

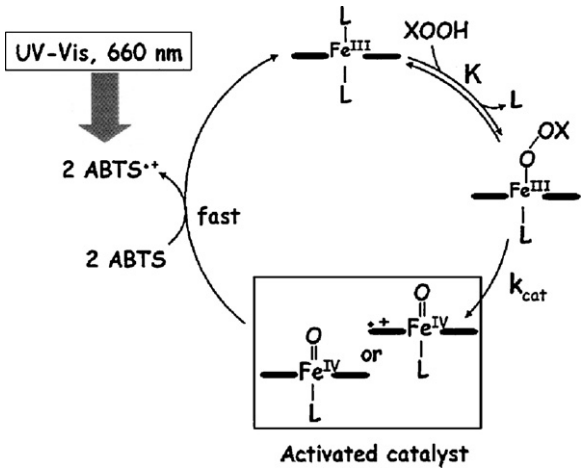

Scheme 2. Catalytic cycle for the oxidation of ABTS.

This objective was not realizable with the TMPS complex, but more progress could be achieved using a high-spin, five-coordinate complex containing an SO_3^- group attached to both a phenyl ring and to the central Fe, see Scheme 3.

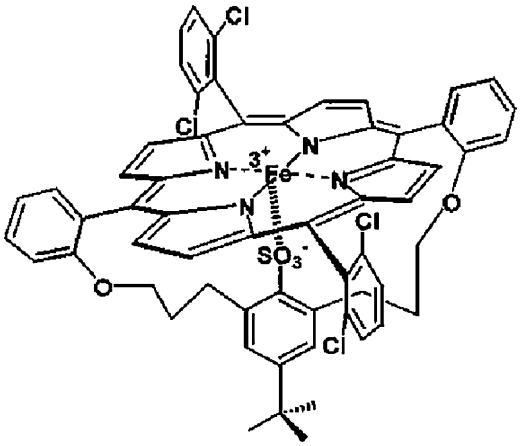

Scheme 3. High-spin five-coordinate complex with SO_3^- group.

Employing *m*-CPBA in acetonitrile (in the absence of substrate), as an oxidant at −35 °C, the rapid reversible coordination of *m*-CPBA to the high-spin Fe(III) center could be monitored. This is represented schematically in Scheme 4.

This step is followed by the rate-determining acid-catalyzed heterolysis of the O–O bond to form the Fe(IV) porphyrin radical cation, in evidence from the spectra shown in Fig. 4 [26].

The primary kinetic data could be analysed to yield values for the coordination step ($k_1 = 4.4 \times 10^3$ mol^{-1} dm^3) and for the rate-determining step ($k_2 = 2.4$ s^{-1}) at −35 °C. The porphyrin radical cation is reasonably stable in the absence of reactive substrates, but is rapidly decomposed upon the addition of *cis*-stilbene with simultaneous regeneration of a very high fraction of the original quantity of the starting Fe(III) complex. A detailed investigation of the cycle was undertaken by combining various designed concentrations of *m*-CPBA, *cis*-stilbene and the starting Fe(III) complex in acetonitrile at −35 °C and monitoring the outcome in the Soret region (412 nm) [26]. The reaction profile is generally of the form of a decrease in absorbance as the starting complex is converted to the porphyrin radical cation, followed by an apparent induction period

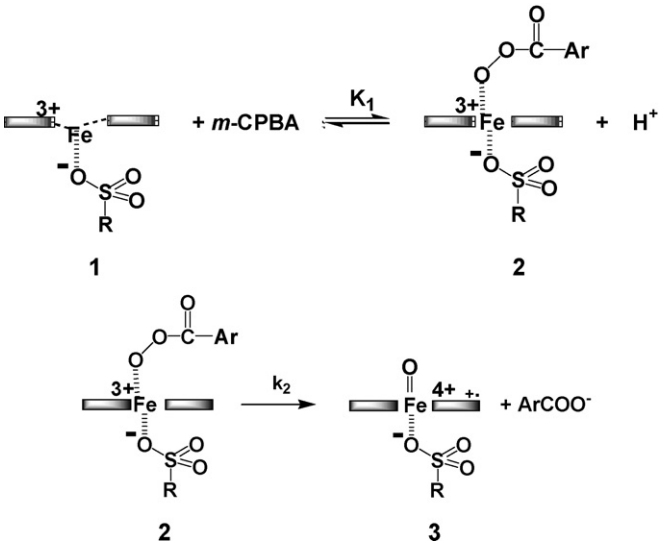

Scheme 4. Reversible coordination of *m*-CPBA to complex **1** in Scheme 3 followed by heterolytic O–O-bond cleavage.

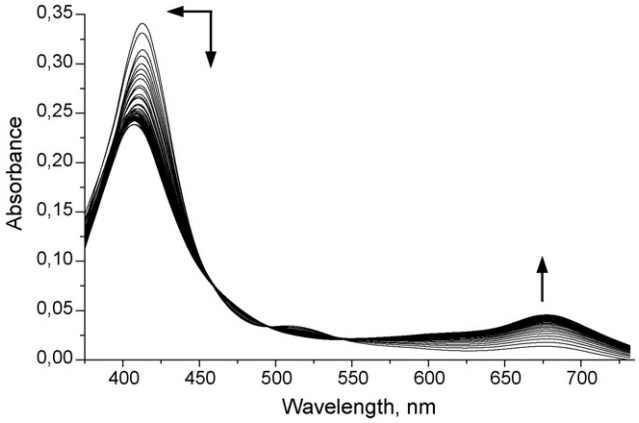

Fig. 4. Formation of ($\mathbf{1}^{\bullet+}$)Fe^{IV}=O in the reaction of **1** with m-CPBA at −35 °C in CH_3CN: rapid-scan spectra [21,23].

that is governed by the excess concentration of the *cis*-stilbene substrate. If the *cis*-stilbene concentration is maintained below a 500-fold excess the pophyrin radical cation is always sufficiently and rapidly regenerated by the 10-fold excess of m-CPBA such that there is no absorbance detected initially at 412 nm. Thus there is a delay in the reformation of the starting complex as shown at various *cis*-stilbene excess concentrations in Fig. 5. The regeneration of the starting complex from the porphyrin cation radical is characterized by a second-order rate constant of 7.0 mol^{-1} dm^3 s^{-1} at −35 °C, obtained from the *cis*-stilbene concentration dependence of the observed rate constant for the re-formation of the starting complex. The kinetic traces for the catalytic cycles could be simulated satisfactorily from the kinetic parameters obtained, and these are shown in Fig. 5. A scheme for the overall catalytic cycle obtained from employing the low-temperature rapid-scan method is displayed (see Scheme 5).

A subsequent study [27] that was stimulated, in part, by the ongoing debate about the role of different species in the oxidation reactions [28,29] used a model porphyrin complex Fe^{III}(TMP), TMP = *meso*-tetramesitylporphyrin. One objective was to compare the relative effectiveness of Fe^{III}(TMP)(*m*-CPBA) and (TMP$^{\bullet+}$)Fe^{IV}=O as catalysts. By appropriate selection of reaction conditions, both

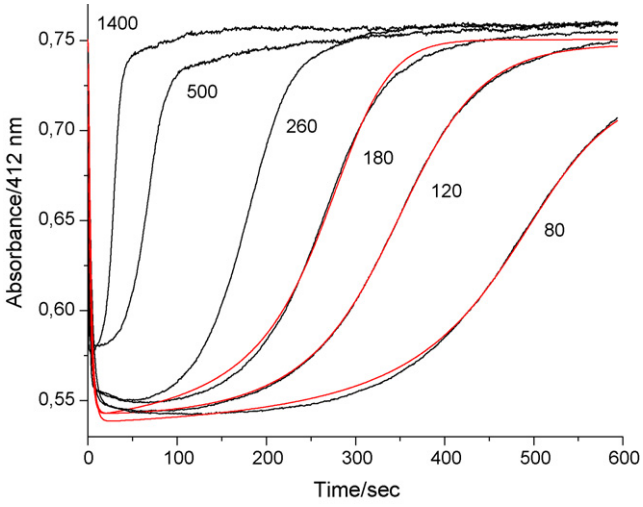

Fig. 5. Typical reaction traces illustrating absorbance changes at 412 nm, at −35 °C, for fixed concentrations of the starting complex, and *m*-CPBA, with varying excess concentrations of *cis*-stilbene, illustrating the variation in the induction period. The red curves were simulated on the basis of the available kinetic data for the reaction steps in Scheme 5 [21,23].

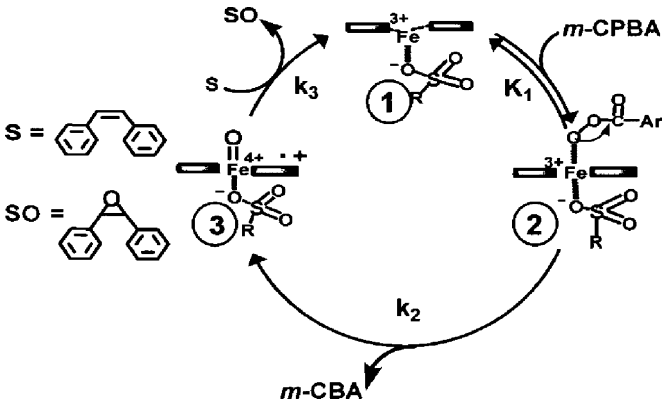

Scheme 5. Overall catalytic cycle (as described in the text).

species could be stabilized at −15 °C in acetonitrile for sufficient time to carry out the epoxidation of *cis*-stilbene and the sulfoxidation of dimethylsulfide. From a thorough analysis of a comprehensive set of kinetics experiments in which concentrations of species were varied widely it could be concluded that the oxygenation capability of the iron(IV) oxoporphyrin π-cation radical is orders of magnitude higher than that of the acylperoxoiron(III) porphyrin complex. This led to the suggestion that the high-valent oxoiron species could be the sole active species responsible for *in vivo* P450 oxygenation reactions.

3.2. Activation of the superoxide ion, $O_2^{\bullet-}$

3.2.1. Manganese(II) complexes

The very rapid (diffusion-controlled) reaction of the superoxide ion with NO, in biological systems to form the peroxynitrite ion ($ONOO^-$) depletes the level of NO and therefore suppresses the beneficial effects of NO [30,31]. Consequently, there is considerable interest in reactions (principally decomposition to dioxygen and hydrogen peroxide) that limit the insidious effect of superoxide. A family of metalloenzymes (superoxide dismutases (SODs)) exists in nature to catalyze the decomposition of superoxide [32]. As there are, at times, various limitations of the application of a SOD as a therapeutic agent in instances of overproduction of superoxide, the development of reagents that function as SOD mimetics is desirable [33]. Considerable effort has been expended to synthesize redox active metal complexes that remove superoxide efficiently and catalytically. It prevails that the most active SOD mimetics are seven-coordinate Mn(II) complexes that possess macrocyclic conformationally flexible ligands, derived from C-substituted pentaazacyclopentadecane [34,35]. Scheme 6 illustrates superoxide dismutation by a metal center.

Of compelling curiosity is how the seven-coordinate geometry of metal complexes favors the remarkable catalytic activity, in some cases exceeding that of a native MnSOD enzyme [36]. In a natural MnSOD the Mn(III) center is surrounded by two histidines and

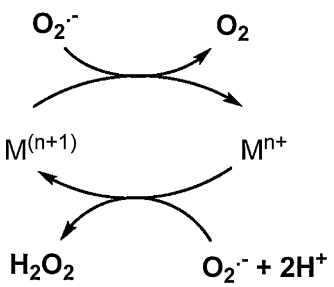

Scheme 6. Superoxide dismutation by a metal center.

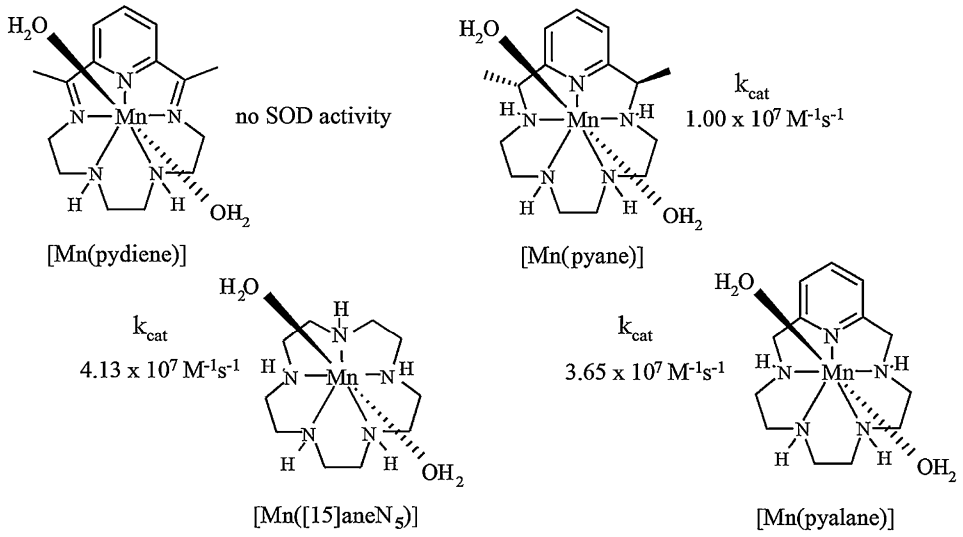

Scheme 7. Seven-coordinate Mn(II) complexes.

one aspartate in an equatorial plane and the trigonal bipyramidal geometry is completed by another histidine and a solvent molecule, probably OH^- in axial positions, a second intriguing property difference between natural and mimetic SOD activity. It has been proposed that the SOD mimetics function in their activity as a result of their pronounced conformational flexibility [37]. Release of a water molecule followed by formation of a six-coordinate intermediate that requires conformational rearrangement of the ligand was proposed as the rate-limiting step in the overall inner-sphere catalytic SOD pathway [36]. To probe the initial phase of the reaction mechanism, measurements of the rates of water exchange on representative Mn(II) complexes were undertaken in an attempt to show whether the rate of water exchange controls substitution reactions and subsequent binding of the superoxide ion [38]. Four seven-coordinate Mn(II) complexes whose rates of water exchange have been determined employing ^{17}O NMR spectroscopy are shown in Scheme 7.

Rate constants for water exchange were generally in the range of $(1–6) \times 10^7\ s^{-1}$ at 25 °C, typically measured in the pH range of 6–11. Thus water exchange is slower than on seven-coordinate $[Mn(EDTA)(H_2O)]^{2-}$ (k_{EX} (25 °C) = $4.4 \times 10^8\ s^{-1}$) [39], but this is readily understood. The increased lability arises from the strong π-donor ability of EDTA and its high negative charge, as well as the fact that in the EDTA complex the water molecule is in the sterically crowded equatorial plane with five donor atoms whereas in the Mn(II) potential SOD mimetics the water molecules are in axial positions. The positive entropies of activation, in the range of +15 to +30 J mol^{-1} K^{-1}, and positive volumes of activation, in the range of +3 to +5 cm^3 mol^{-1} for the water exchange reaction on the seven-coordinate, Mn(II) SOD mimetic complexes suggest a dissociative interchange (I_d) mechanism, in contrast to the I_a mechanism for hexaaqua Mn(II) ions ($\Delta V^{\neq} = -5.4$ cm^3 mol^{-1}) [40]. A previous effort to correlate the inner-sphere SOD catalytic rate constants with the water exchange rate constant for $Mn_{(aq)}^{II}$ did not withstand scrutiny [41]. The k_{EX} values for water exchange on the seven-coordinate SOD mimetic complexes vary over at least half an order of magnitude and when corrected to compare with the second-order rate constant for dismutation of superoxide indicated that they are significantly lower. It was therefore argued that water release is not the rate-determining step, and a substitution mechanism in which the incoming superoxide plays a role, and an eight-coordinate transition state was invoked [21]. It was therefore concluded from these results, and other analysis that conformational flexibility of a pentadentate ligand is not a mandatory requirement at all, as in the proposed interchange mechanism this ligand can remain in its planar conformation [42].

3.2.2. Iron-porphyrin complexes

The superoxide ion can be subject to dismutation by some, but by no means all iron-porphyrin complexes [43,44]. The biochemistry of dioxygen, and both its superoxide and peroxide forms is related to the iron-porphyrin centers in different hemoproteins. Both iron(III)-superoxo and iron(III)-peroxo species are involved in the transport of oxygen and in the catalytic cycle of the monoxygenase enzyme, cytochrome P450 [45–49]. The general subject area of iron-porphyrin complexes and related peroxo complexes has been investigated thoroughly, and has also been reviewed [45,48–51]. Recounting the relevant literature is not within the scope of this contribution. However, it is important to note that it has been established that in aprotic coordinating solvents (DMSO, CH_3CN for example) 1 equivalent of KO_2 reduces Fe(III)-porphyrins to Fe(II), whereas an additional equivalent of KO_2 produces an Fe(III)-peroxo-porphyrin species, see Eqs. (1) and (2) [52,53].

$$[Fe^{III}(porphyrin)]^+ + O_2^{\bullet -} \rightleftarrows [Fe^{II}(porphyrin)]^+ + O_2 \quad (1)$$

$$[Fe^{II}(porphyrin)]^+ + O_2^{\bullet -} \rightleftarrows [Fe^{III}(porphyrin)(O_2^{2-})]^- \quad (2)$$

The focus here will be on a specific novel complex, the Fe(III) complex of a crown ether-porphyrin conjugate (H_2porph) and its interaction with superoxide ion [54], with the expectation that the reaction scheme of equations will be followed (see Scheme 8).

The complex was characterized by X-ray diffraction, yielding the crystal structure, Mössbauer spectroscopy and IR and NMR spectroscopy. In DMSO solution the reaction of $[Fe^{III}(Porph)(DMSO)_2]^+$ with KO_2 was investigated. A first reaction step that involved reduction to form $[Fe^{II}(Porph)(DMSO)_2]$ was not examined in detail kinetically because monitoring it was compromised by the parallel formation of an Fe(III)-hydroxo species. However, the kinetics and thermodynamics of a second step, reversible binding of the superoxide ion to the Fe(II) complex and formation of an Fe(III)-peroxo species were studied in detail by a stopped-flow method, with high speed diode array detection capability, exploiting UV/vis absorbance differences, at 25 °C. The forward rate constant was 3.7×10^4 mol^{-1} dm^3 s^{-1}, and the reverse rate constant was 0.21 s^{-1}. The equilibrium constant for the reversible binding of superoxide was obtained independently of the method using the ratio of the kinetically derived parameters, and good agreement was found between the values. In a mixed DMSO/CH_3CN medium the kinetics

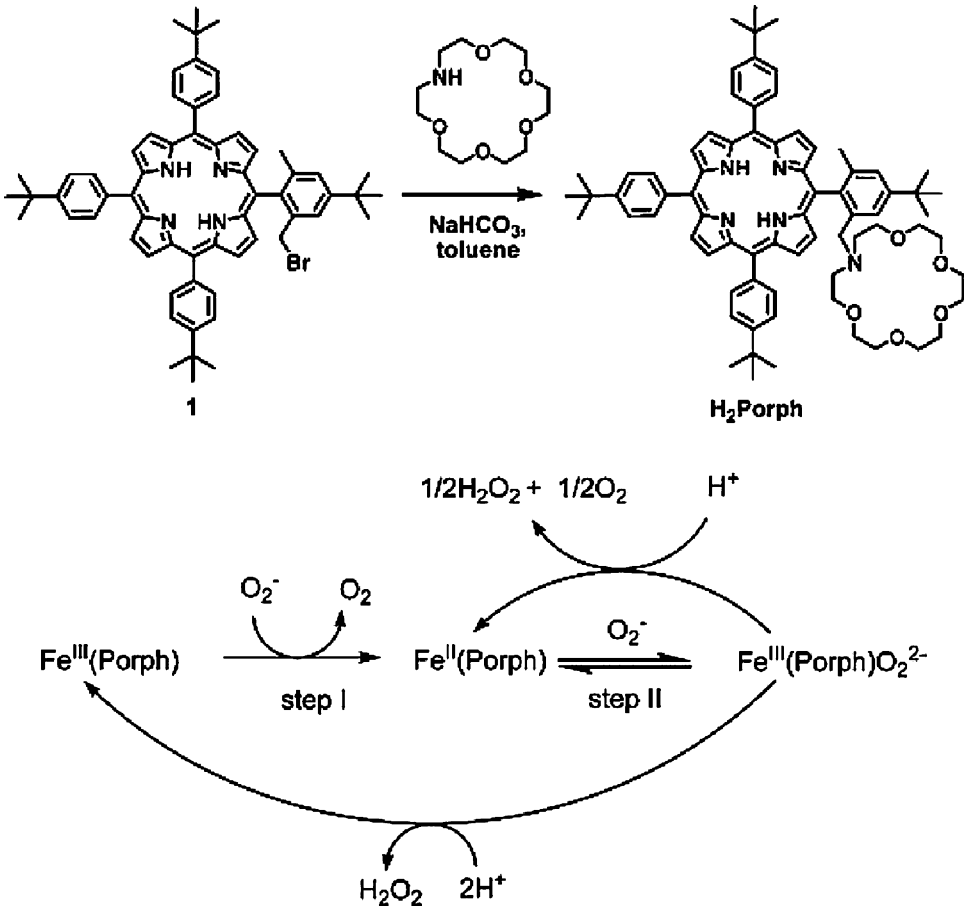

Scheme 8. Preparation of the crown ether-porphyrin and overall reaction scheme based on reactions (1) and (2) [54].

of binding of superoxide to $[Fe^{II}(Porph)(DMSO)_2]$ could be monitored over the temperature range −40 °C to +25 °C, yielding for the forward reaction $\Delta H^{\neq}$ of 61 kJ mol^{-1} and $\Delta S^{\neq}$ of +48 J mol^{-1} K^{-1}. The positive value of $\Delta S^{\neq}$ suggests that the rate-determining step is dissociative in nature. An analysis of the individual steps in Eqs. (3) and (4) led to the conclusion that formation of the transition state en route to a five-coordinate intermediate by loss of DMSO is the rate-determining step.

$$[Fe^{II}(Porph)(DMSO)_2] \rightleftarrows [Fe^{II}(Porph)(DMSO)] + DMSO \quad (3)$$

$$[Fe^{II}(Porph)(DMSO)] + O_2^{\bullet -} \rightleftarrows [Fe^{III}(Porph)(DMSO)(O_2^{2-})] \quad (4)$$

It prevails, of course, that the experimentally determined entropy of activation is a composite value; that is the somewhat larger positive value expected in the former forward reaction is offset by a contrary (expected negative) value in the second forward reaction. The significance of this reaction between the crown ether-porphyrin Fe(III) complex and superoxide (with focus only on the second reaction) is that it is experimentally, technically demanding, requiring creative experimental design, and is the first time such a reaction has been characterized successfully kinetically and thermodynamically. The possible relevance of these results for events in physiological conditions can be accessed through references [21,54] and other cited literature therein.

3.3. Dioxygen binding and activation by model copper(I) complexes

There is a vast body of literature on dioxygen binding by copper(I) complexes that model the copper-containing proteins that are capable of activating or transporting O_2. There are examples of complexes that model mononuclear sites, but also a considerable number of dicopper complexes and indeed trinuclear copper complexes. A selection of valuable starting points for subject familiarisation is provided [55–60]. Some of the reaction steps involved in these studies are extremely rapid at ambient temperature. Therefore, low-temperature methods are frequently employed to characterise the kinetics processes and establish the UV/vis spectra of intermediate species. This is not a new development and an overview of low-temperature methods in addressing the kinetics and thermodynamics of copper(I) dioxygen interactions has been provided [61]. In another early study, low-temperature (−20 °C in acetone) was combined with a range of elevated hydrostatic pressures to not only obtain a kinetics profile of a copper(I) complex in its interaction with dioxygen to form a dinuclear copper-peroxo complex, but also to establish the transition state position in a relative partial molar volume status [62]. It prevailed that the species forming between the two reactants had a combined partial molar volume of 15 cm^3 mol^{-1} less that the reactants themselves. The use of hydrostatic pressure as an experimental parameter in kinetics investigations of solution reactions has been presented in considerable detail [63] and therefore the background, experimental aspects and illustrative examples of the mechanistic value will not be repeated here. Furthermore, except in special cases, one of which is referred to above, combining low-temperature rapid flow methods with elevated pressures is technically infeasible at present. A comprehensive account of how to conduct low low-temperature, rapid scan, stopped-flow experiments, with examples, has been provided [64].

In this article it is only possible to present a very limited, but interestingly illustrative selection of investigations from the vast number of reports on the overall subject.

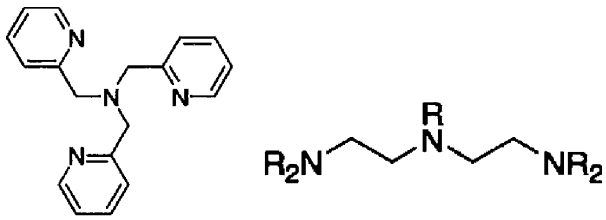

TMPA Me5dien (R = Me)

Scheme 9. Structures of the chelates TMPA and Me_5dien.

3.3.1. Mononuclear copper(I) model complexes

The structure and design features of ligands that can form copper(I) complexes that are then able to bind and activate molecular oxygen that is subsequently cleaved and leads to consecutive attack on a substrate have occupied many investigators. Detecting and characterizing species along the pathway and establishing kinetic parameters and thermodynamic properties of each step are important goals that can lead to a thorough mechanistic understanding; however, this overall objective is often not fully realized. Of many possible approaches using different ligands, only a few can be included here. Use of the tripodal tetradentate ligand TMPA (tris(2-pyridylmethyl)amine) (see Scheme 9) yielded a stabilized *trans*-peroxo copper complex and this led to a dinuclear copper(II) peroxo complex being characterized crystallographically. In addition, simple bidentate and terdentate open-chain ligands have also been used to form copper(I) complexes and then to investigate the reactivity between these complexes and dioxygen. As an illustration of a typical investigation, the reaction of dioxygen with the copper(I) complex of the terdentate ligand 1,1,4,7,7-pentamethyldiethylenetriamine (Me_5dien, Scheme 9), as monitored using a low-temperature stopped-flow method is described [65].

The copper(I) complex of Me_5dien was formed *in situ* in the stopped-flow instrument and reacted therein with dioxygen in acetone solution at various temperatures in the range of −35 to −90 °C. Spectra were recorded in the wavelength range from 320 to 500 nm, or absorbance time traces where maximum absorbance change occurred (404 nm in this case) were acquired. Very similar time-resolved UV/vis spectra were displayed for reaction of $[Cu(Me_5dien)(CH_3CN)]ClO_4$ with dioxygen in propionitrile solution. Based upon the UV/vis spectra the complex formed was proposed to be an bis(μ-oxo)dicopper(III) species, although confirmation could be not achieved as the stability of the complex was insufficient for resonance Raman measurements to be successful. A reaction scheme, based upon the results of themselves and the kinetic studies of others [66] was outlined (Eqs. (5)–(7)) for the complex containing coordinated acetonitrile.

$$[Cu(Me_5dien)(CH_3CN)]^+ + O_2 \rightleftarrows [Cu(Me_5dien)(O_2)]^+ + CH_3CN \quad (5)$$

$$[Cu(Me_5dien)(O_2)]^+ + [Cu(Me_5dien)(CH_3CN)]^+ \rightleftarrows [\{Cu(Me_5dien)\}_2(\mu\text{-}O)_2]^{2+} + CH_3CN \quad (6)$$

$$[\{Cu(Me_5dien)\}_2(\mu\text{-}O)_2]^{2+} \rightarrow \text{decomposition} \quad (7)$$

Since there is significant decay of the bis(μ-oxo) complex and a rapid back reaction, the complex does not accumulate. It was argued that although the adduct formation must be stepwise via a mononuclear superoxo complex, the kinetic data could be fitted with a simpler scheme that did not include such a reactive intermediate, and that had been employed earlier [67,68]. The program *specfit* was applied successfully to the following scheme (Eqs. (8) and (9)).

$$[Cu(Me_5dien)(CH_3CN)]^+ + O_2 \rightleftarrows [\{Cu(Me_5dien)\}_2(\mu\text{-}O)_2]^{2+} + CH_3CN \qquad k_1/k_{-1} \quad (8)$$

$$[\{Cu(Me_5dien)\}_2(\mu\text{-}O)_2]^{2+} \rightarrow \text{decomposition} \qquad k_2 \quad (9)$$

The analysis, with the assumption that $[Cu(Me_5dien)(CH_3CN)]^+$ and $[\{Cu(Me_5dien)\}_2(\mu\text{-}O)_2]^{2+}$ are the spectroscopically active species, yielded values for k_1, k_{-1} and k_2, and with these kinetic parameters being determined over a range of low temperatures, the thermal activation parameters could also be extracted. These results were assembled and compared and contrasted with those for similar reactions of dioxygen with Cu(I) complexes. One significant finding was the reaction of dioxygen with $[Cu(Me_5dien)(CH_3CN)]^+$ was much faster than that of other complexes, but this was thought to arise from a different chelate ring size; many other complexes are six-membered chelate complexes that are regarded as stabilizing copper(I) complexes [69]. Contrary to expectation, copper(I) complexes of related ligands (Et_5dien, Mebpa, MeL) (Scheme 10) to Me_5dien, showed no detectable reactivity or formation of dinuclear bis(μ-oxo)copper complex formation upon interaction with dioxygen.

Thus it is evident that much remains to be understood regarding the exact ligand composition, dentate number, potential chelate ring size and other properties that give rise to formation of a dinuclear copper adduct upon reacting the relevant copper(I) complex with molecular oxygen.

The dinuclear copper(I) complex, $([Cu_2(APME)_2](ClO_4)_2$, where APME = 2-aminoethyl(2-pyridylmethyl)-1,2-ethanediamine and is a mixed aliphatic/aromatic tetradentate, tripodal ligand, has been synthesized. It was interacted with dioxygen, and time-resolved, low-temperature spectra show the formation of an adduct, an oxidation product that was obtained at about −90 °C in either CH_2Cl_2 or in acetone [70]. The choice of APME to form a complex was directed, in part, by previous success in forming the superoxo complex $[Cu(TMPA)(O_2)]^+$, prior to formation of $[Cu_2(TMPA)_2(O_2)]^{2+}$ [71,72], and using tren as a ligand in similar studies [73,74]. However, complete kinetic characterization of formation of the oxygen adduct from the reaction of the dinuclear complex of APME has not been realized, although potential relevance to the copper-containing enzyme, peptidylglycine-α-hydroxylating monooxygenase was noted.

3.3.2. Dicopper(I) complexes containing podand-type Schiff-base ligands

Hemocyanin, catechol oxidase and tyrosinase are examples of proteins that possess the capability of activating or transporting dioxygen by means of a synergistic process involving two copper ions [55,56]. One approach to begin to understand the mechanism by which a dicopper site binds and/or activates O_2 is to model O_2-processing proteins with synthetic copper complexes. Some studies have used mononuclear copper complexes that upon exposure to oxygen self-assemble into a binuclear copper species [57–60]. Another approach has been to design ligands that can complex two copper(I) centers and examine the interaction of the complex with O_2 [68]. The selection of ligands, the ligands and dicopper(I) preparations and their extensive characterizations have been reported (see Scheme 11).

1X is a complex with a Schiff-base ligand containing two terdentate copper binding sites and linked by a xylyl spacer, and X can be various counter ions. This arrangement is an aim to reproduce structural aspects of the active site of some dicopper proteins. The complex, **1X** and others prepared were found to bind O_2 very rapidly. Computational and spectroscopic studies on

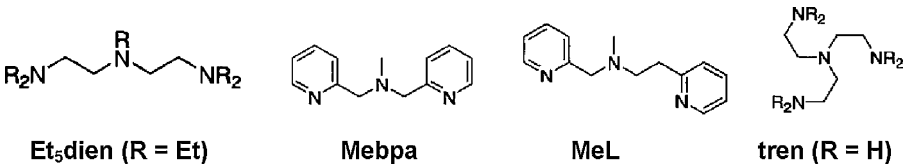

Scheme 10. Structures of the chelates Et_5dien, Mebpa, MeL and tren.

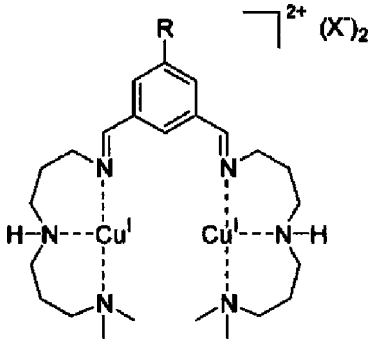

Scheme 11. The dicopper(I) complex, $[Cu_2^I(^HL)]X_2$, = **1X**, R = H.

the nature of the metastable oxygenated intermediates formed, showed that their structure and nuclearity were dependent on solvent and counter ion. A kinetics investigation of the interaction of **1X** with O_2 in acetone (X = $CF_3SO_3^-$ and BArF, where BArF = [B(3,5-$(CF_3)_2C_6H_3)_4$]$^-$) was undertaken [75]. The rapidity of the reactions necessitated employment of a stopped-flow instrument in low-temperature (−20 to −80 °C) mode, in either single wavelength or rapid-scan applications. As the oxygenation reaction rates were essentially the same, independent of anion, a detailed examination of the kinetics was pursued only for **1**BArF. Rapid accumulation of the bis-μ-oxo species **1**(O_2)BArF occurs, followed by its decomposition. In the two-phase reaction sequence, the second reaction is much slower allowing the former step to be readily characterized kinetically. Analysis of the primary kinetic data showed that the reaction was second-order overall, first-order in each of the dicopper complex and the O_2 concentrations, with a rate constant of 3.84×10^3 mol^{-1} dm^3 s^{-1} at −80 °C. This represents a three orders of magnitude more rapid oxygenation reaction than for the xylyl bridged $[Cu_2^I(m\text{-}XYL^{MeAN})]^{2+}$ species (see Scheme 12).

The difference originates from a smaller activation enthalpy (4.9 kJ mol^{-1}) and less negative activation entropy (−148 J mol^{-1} K^{-1}) for reaction of **1**BArF. The corresponding values for oxygenation of $[Cu_2^I(m\text{-}XYL^{MeAN})]^{2+}$ are 9.5 kJ mol^{-1} and −175 J mol^{-1} K^{-1}. It was proposed that the fast reaction here arises from relatively high preorganisation conferred by the more rigid imine N group in comparison with tertiary amines in the corresponding location within the ligand. In addition, there is a possible hemilability of the imine group that may lower the coordination number of the Cu ion, enhancing its reactivity. It was also suggested that the presence of the N–H group may stabilize O_2 binding to the first Cu ion by H-bonding or via better stabilization of the Cu^{II} or Cu^{III} oxidation state. An analysis of the possible mechanistic scenarios that would be compatible with the rate law and with other oxygenation kinetic parameters for other dicopper complexes led to the conclusion that a synergistic role of the copper ions in O_2 binding and activation is established for this reaction.

Finally in this section attention is drawn to the potential for future kinetics investigations at low temperatures on a range of copper–oxygen systems, as spectroscopic (UV/vis principally) characterizations of labile species, typically at −80 °C, have been reported recently [76].

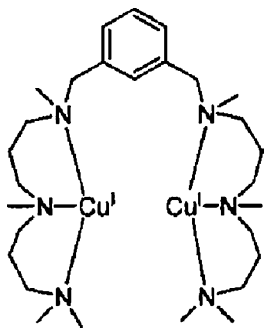

Scheme 12. The complex $[Cu_2^I(m\text{-}XYL^{MeAN})]^{2+}$.

3.4. Dioxygen activation at non-heme iron

Iron may also be a prominent key elemental component of metal-based compounds involved in dioxygen binding and activation for efficient and selective organic substrate oxidation processes. In particular iron-containing, metalloenzymes, for example, iron oxidases and oxygenases are associated with iron-peroxo or high-valent iron-oxo intermediates in the context of oxygen activation. A wide-ranging background of the synthetic, spectroscopic, structural and computational aspects of various iron-based model compounds and the intermediates generated has been provided [77,78]. These reports are in most cases supplying necessary information for planning more detailed kinetic and mechanistic investigations of the formation and reactivity of various non-heme iron-peroxo and iron-oxo intermediates. Again cryogenic stopped-flow methods are central to the goal of detection and characterization of rapidly accumulating, and decaying intermediates [79,80]. It prevails that in some examples the subsequent substrate oxidation reactions are detectable at ambient temperatures. Many of the ligands that have been employed in iron complexes used for oxygen activation have been assembled [80].

3.4.1. Reaction of a mononuclear iron complex with O_2

A pentaaza macrocyclic ligand, H_2pydioneN_5, forms high-spin iron(II) and iron(III) complexes (see Scheme 13). The ligand selection was prompted because it was reasoned that the intermediates would be biologically relevant, i.e. analogous to porphyrin systems [81].

The di-deprotonated iron(II) complex, Fe(pydioneN_5), reacts rapidly with oxygen in a 8% DMF/CH_3CN solution, as detected spectroscopically at −40 °C, forming initially an iron(III) superoxo species and subsequently a di-iron(III)-peroxo species. Later a

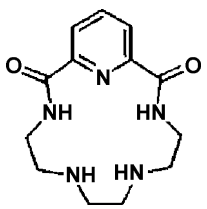

Scheme 13. The chelate H_2pydioneN_5.

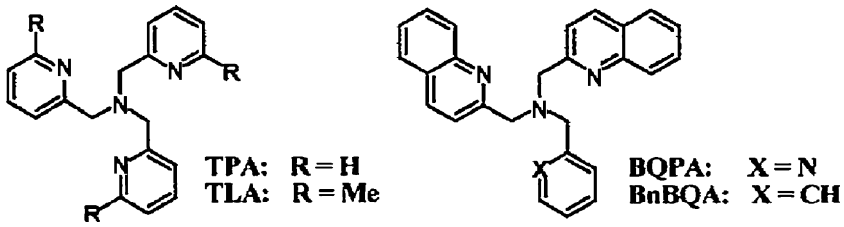

Scheme 14. The chelates TPA, TLA, BnBQA and BQPA.

decomposition product could be detected. In methanol the kinetics were different and an intermediate was not detected spectroscopically. A similar situation prevailed for the oxygenation reaction for the mono-deprotonated complex Fe(HpydioneN$_5$). Clearly the presence of an accessible proton in the vicinity of the reaction center or from the solvent changes the oxygenation pathway.

3.4.2. Reaction of a dinuclear iron(II) complex with O_2

It is important before citing some individual studies to recognize the pioneering and on-going investigations of the Lippard group on dioxygen activation at non-heme di-iron complexes. These studies have involved synthetic models, structural and spectroscopic characterizations as well as mechanistic investigations, and representative publications are cited [82]. The kinetics of oxygenation of several non-heme di-iron(II) complexes have been investigated [83–86]. A key aspect of these studies is to understand the combination of ligands and coordination arrangements that lead to complexes that are effective in subsequent substrate oxidation reactions. A tabulation of kinetic and activation parameters shows a dramatic range of second-order (first-order in both di-iron(II) complex and oxygen concentrations) rate constants (ca. 1 mol^{-1} dm^3 to 7×10^4 mol^{-1} dm^3) for the dioxygen reaction, collated at −40 °C. Typically the solvent was CH_2Cl_2 or CH_3CN. Enthalpies of activation are low, but entropies of activation are markedly negative, an expectation for an associative process. For the purpose of further discussion a selection of dihydroxo bridged di-iron(II) complexes $[Fe_2(OH)_2(L)_2]^{2+}$ is chosen (L = TPA, TLA, BnBQA, BQPA, see Scheme 14).

An analysis pointed to the initial formation of a di-iron-superoxo intermediate, and in fact observation of such an intermediate in the oxygenation reaction of $[Fe_2(OH)_2(TLA)_2]^{2+}$ at −80 °C was reported [87]. Because the kinetic properties did not correlate with the redox potentials of the di-iron(II) complexes it was proposed that rates of ligand substitution rather than electron-transfer rates limited the O_2 binding rates [86]. Steric hindrance around the iron coordination sites, for example in the TLA complex, protected the peroxo intermediate from oxidative decomposition, but also is responsible for slow oxygenation rates. However, the situation is not completely straightforward as the less sterically hindered TPA complex is also not rapidly oxygenated [88]. It was proposed that this could be explained by a more compact and symmetric $Fe_2(OH)_2$ core for the latter complex requiring a higher enthalpy of activation (as observed) and lower entropy of activation (also as observed) to break shorter Fe-O(H) and/or Fe-N(py) bonds in the course of oxygen binding.

Facile acceleration of oxygenation was accomplished by three orders of magnitude by using the complex containing a vacant coordination site, $[Fe_2(OH)_2(BnBQA)_2]^{2+}$, by the simple expedient of replacing one pyridine arm of the BQPA analogue by a phenyl moiety [86]. The effects of addition of non-coordinating bases, and of protonation and deprotonation on the oxygenation reactions of these complexes have been investigated, with a view to optimizing substrate oxidation reactions and preventing unproductive reaction pathways involving the starting iron complex species [86]. It was also noted that a dinucleating ligand that provides three N donors at each iron, two additional sites at each iron are occupied by bridging oxygen atoms from a carboxylate moiety, form complexes that also react rapidly with dioxygen, a finding also related to coordination unsaturation [85].

These oxygenation reaction studies are a prelude to the use of the iron(III)-peroxo intermediates in substrate oxidation, and also reactions involving hydrogen peroxide. For example, di-iron(III)-TPA complexes with H_2O_2 yield a hydroperoxo intermediate that oxidises phosphines and phenols, and in addition catalytic olefin epoxidation and inner-sphere stoichiometric selective aromatic *ortho*-hydroxylation has been demonstrated using a combination of coordinatively unsaturated iron complex containing aminopyridine ligands [89]. The multi-step reaction schemes relating to oxidation reactions of substrates are complex, but full kinetic characterization has been accomplished in many systems.

3.5. Carbon–hydrogen bond activation by platinum(II) complexes

It will be shown that enlightenment regarding the mechanism of the reaction implied by this sub-heading will be achieved by study of the reverse reaction. It has been recognized for a considerable time that development of direct, selective methods for catalytic conversion of hydrocarbons to products of enhanced value is a key goal for chemists. A vast literature on this complex subject, particularly the activation of C–H bonds in hydrocarbons, has developed [90–92]. Some aqueous Pt^{II} salts have been shown to activate C–H bonds in alkanes and arenes. Of the many possible approaches, one that is aided by using low-temperature, scanning stopped-flow spectrophotometry, uses a model complex, (N–N)PtR_2, where N–N is a diimine ligand (N–N = ArN=C(Me)–C(Me)=NAr, where Ar = 2,6-$Me_2C_6H_3$), and R represents a hydrocarbon group. A vital issue in the overall activation process is whether the proton to be removed from the hydrocarbon dissociates directly from an activated metal–hydrocarbon complex (termed a σ-complex), or from a hydrido-ligand that is formed via oxidative cleavage of the C–H bond of the σ-complex intermediate (see Scheme 15) [93,94].

An attempt to answer this question was based upon monitoring the reaction following isotopic substitution. However, because isotopic scrambling occurred, this approach was unfruitful. It was decided therefore, that since resolution of the mechanism in the forward direction had not been successful, to study the reac-

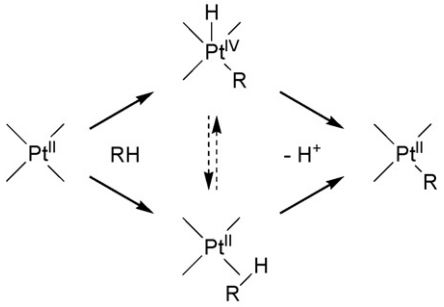

Scheme 15. Possible pathways for proton removal in C–H bond activation.

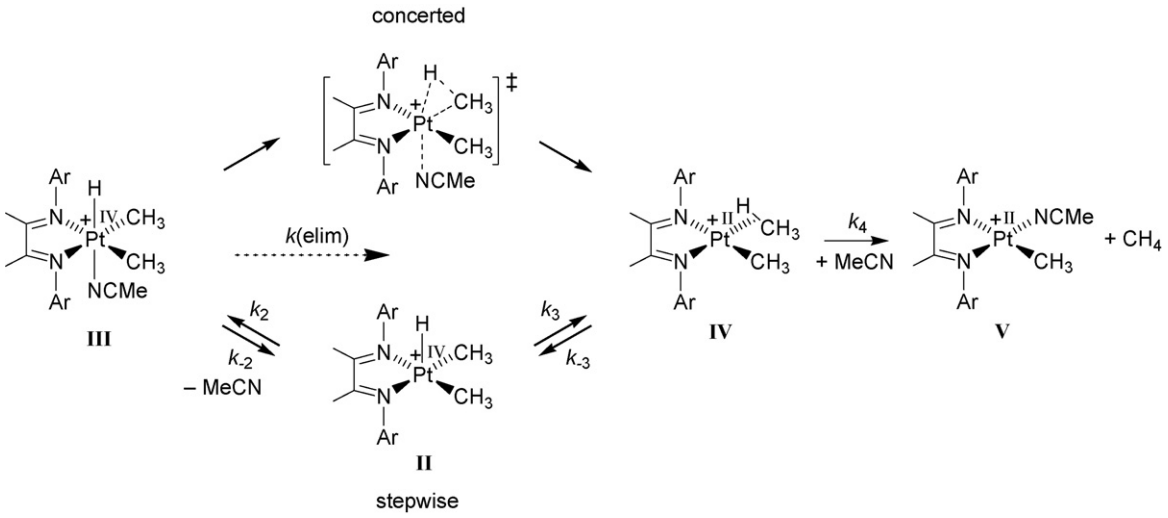

Scheme 16. Steps in the protonation and release of methane.

tion in the reverse direction and thereby infer the mechanism for the forward direction [95]. Accordingly a detailed kinetic study of the protonation and subsequent reductive elimination of the (N–N)PtR_2 complex in dichloromethane was undertaken. The protonation step is very rapid, hence the need for a low-temperature method to enable kinetic data to be acquired is apparent. The effects of acid ($HBF_4{\cdot}Et_2O$) concentration, a coordinating solvent (CH_3CN) and temperature on the kinetics of the protonation step were analysed. A second-order rate constant at −78 °C of 1.52×10^4 mol^{-1} dm^3 s^{-1} was derived, and the relevant activation parameters, $\Delta H^{\neq} = 15.2$ kJ mol^{-1} and $\Delta S^{\neq} = -85$ J mol^{-1} K^{-1} were determined. These parameters are consistent with a mechanism in which addition of a proton to the Pt^{II} compound results in the formation of a hexacoordinate platinum(IV)hydrido intermediate in a stepwise process rather than a concerted process. Protonation of a metal center is not common and the fact that this is compatible with the experimental findings is a significant aspect of this investigation. The second step, release of methane, is accessible kinetically at temperatures closer to ambient, and the activation parameters obtained from kinetics measurements are $\Delta H^{\neq} = 75$ kJ mol^{-1}, $\Delta S^{\neq} = +38$ J mol^{-1} K^{-1} and $\Delta V^{\neq} = +18$ cm^3 mol^{-1}, values that are compatible with a dissociative mechanism. The departing methane dissociates from the hexacoordinate Pt^{IV} species and a pentacoordinate intermediate is formed (see Scheme 16; complete details of the significance and magnitudes of the rate constants in the scheme and the arguments relating to each of the numbered species are contained in reference [95]).

Relevant, earlier NMR spectroscopic measurements could be invoked [96] to illustrate consistency with the mechanistic details of the low-temperature investigation.

4. Concluding comment

Insight into reaction mechanisms obtained from kinetics studies reported herein would not be available without resort to the low-temperature modification of the stopped-flow technique. A very diverse set of examples from different areas of chemistry has been used to illustrate succinctly the value of this expedient method.

Acknowledgements

The authors of this article have the honor to have the opportunity to provide a contribution to celebrate the occasion of Professor Pearson's 90th birthday. The technical skill and interpretative excellence of the research endeavors of the authors cited in the references are recognized. Professor Edward F. Caldin and colleagues at the Universities of Leeds and Kent in Canterbury, were the principal investigators in the original development of the low-temperature stopped-flow method. The financial support for research reported from our laboratories comes from the Deutsche Forschungsgemeinschaft through SFB 583 and SPP1118, and the Volkswagen Foundation, and that support is greatly appreciated.

References

[1] A.A. Frost, R.G. Pearson, Kinetics and Mechanism, A Study of Homogeneous Chemical Reactions, John Wiley and Sons, New York, 1953;
A.A. Frost, R.G. Pearson, Kinetics and Mechanism, A Study of Homogeneous Chemical Reactions, 2nd ed., John Wiley and Sons, New York, 1961;
J.W. Moore, R.G. Pearson, Kinetics and Mechanism, A Study of Homogeneous Chemical Reactions, 3rd ed., Wiley-Interscience, New York, 1981.
[2] F. Basolo, R.G. Pearson, Mechanisms of Inorganic Reactions, A Study of Metal Complexes in Solution, John Wiley and Sons, New York, 1958;
F. Basolo, R.G. Pearson, Mechanisms of Inorganic Reactions, A Study of Metal Complexes in Solution, 2nd ed., John Wiley and Sons, New York, 1967.
[3] E.F. Caldin, Fast Reactions in Solution, Blackwell Scientific Publications, Oxford, 1964.
[4] M. Eigen, L. de Maeyer, in: S.L. Friess, E.S. Lewis, A. Weissberger (Eds.), Investigations of Rates and Mechanisms of Reactions, 2nd. ed., Interscience, 1963.
[5] G. Porter, in: S.L. Friess, E.S. Lewis, A. Weissberger (Eds.), Investigations of Rates and Mechanisms of Reactions, 2nd ed., Interscience, 1963.
[6] R.G. Pearson, Chemical Hardness, John Wiley-VCH, Weinheim, 1997.
[7] R.G. Pearson, J. Chem. Sci. 117 (2005) 369.
[8] E.F. Caldin, The Mechanisms of Fast Reactions in Solution, IOS Press, Oxford, 2001.
[9] Q.H. Gibson, Prog. Biophys. 9 (1959) 1;
Q.H. Gibson, L. Milnes, Biochem. J. 91 (1964) 161.
[10] M. Eigen, G.G. Hammes, Adv. Enzymol. 25 (1963) 1.
[11] H. Gutfreund, An Introduction to the Study of Enzymes, Blackwell Scientific Publications, Oxford, 1965 (Chapter IV).
[12] R.G. Pearson, R.E. Meeker, F. Basolo, J. Am. Chem. Soc. 78 (1956) 709.
[13] R.G. Pearson, R.L. Dillon, J. Am. Chem. Soc. 75 (1953) 2439.
[14] R.G. Pearson, L.H. Piette, J. Am. Chem. Soc. 76 (1954) 3087.
[15] E.F. Caldin, M. Trickett, Trans. Faraday Soc. 49 (1953) 772;
C.R. Allen, A.J.W. Brook, Trans. Faraday Soc. 56 (1960) 788;
J.B. Ainscough, E.F. Caldin, J. Chem. Soc. (1960) 2411.
[16] R.P. Bell, The Proton in Chemistry, Methuen, 1959.
[17] A. Jarczewski, C.D. Hubbard, J. Mol. Struct. 649 (2003) 287.
[18] E.F. Caldin, J.E. Crooks, A. Queen, J. Phys. E: Sci. Instrum. 6 (1973) 930.
[19] TgK Scientific Limited, 7, Long's Yard, St. Margaret's Street, Bradford on Avon, Wiltshire BA15 1DH, UK. TedK@tgkscientific.com.
[20] Bio-Logic Science Instruments SAS, 1, Rue de L'Europe, Claix FR-38640, France.
[21] I. Ivanović-Burmazović, R. van Eldik, Dalton Trans. (2008) 5259.
[22] A. Franke, G. Stochel, C. Jung, R. van Eldik, J. Am. Chem. Soc. 126 (2004) 4181.
[23] A. Franke, N. Hessenauer-Ilicheva, D. Meyer, G. Stochel, W.-D. Woggon, R. van Eldik, J. Am. Chem. Soc. 128 (2006) 13611.
[24] W.-D. Woggon, Acc. Chem. Res. 38 (2005) 127.
[25] M. Wolak, R. van Eldik, Chem. Eur. J. 13 (2007) 4873.

[26] N. Hessenauer-Ilicheva, A. Franke, D. Meyer, W.-D. Woggon, R. van Eldik, J. Am. Chem. Soc. 129 (2007) 12473.
[27] A. Franke, C. Fertinger, R. van Eldik, Angew. Chem. Int. Ed. 47 (2008) 5238.
[28] M.J. Cryle, J.J. de Vos, Angew. Chem. Int. Ed. 45 (2006) 8221.
[29] C. Li, L. Zhang, H. Hirao, W. Wu, S. Shaik, Angew. Chem. 119 (2007) 8316.
[30] T. Nauser, W.H. Koppenol, J. Phys. Chem. A 106 (2002) 4084.
[31] R. Radi, G. Peluffo, M.N. Alvarez, M. Naviliat, A. Cayota, Free Radic. Biol. Med. 30 (2001) 463.
[32] D.P. Barondeau, C.J. Kassmann, C.K. Bruns, J.A. Tainer, E.D. Getzoff, Biochemistry 43 (2004) 8038.
[33] D.P. Riley, Chem. Rev. 99 (1999) 2573.
[34] C. Muscoli, S. Cuzzocrea, D.P. Riley, J.L. Zweier, C. Thiemermann, Z.-Q. Wang, D. Salvemini, Br. J. Pharmacol. 140 (2003) 445.
[35] D. Salvemini, Z.-Q. Wang, J.L. Zweier, A. Samouilov, H. Macarthur, T.P. Misko, M.G. Currie, S. Cuzzocrea, J.A. Sikorski, D.P. Riley, Science 286 (1999) 304.
[36] K. Aston, N. Rath, A. Nauk, U. Slomczynska, O.F. Schall, D.P. Riley, Inorg. Chem. 40 (2001) 1779.
[37] D.P. Riley, O.F. Schall, Adv. Inorg. Chem. 59 (2007) 233.
[38] A. Dees, A. Zahl, R. Puchta, N.J.R. van Eikema Hommes, F.W. Heinemann, I. Ivanović-Burmazović, Inorg. Chem. 46 (2007) 2459.
[39] M.S. Zetter, M.W. Grant, E.J. Wood, H.W. Dodgen, J.P. Hunt, Inorg. Chem. 11 (1972) 2701.
[40] Y. Ducommun, K.E. Newman, A.E. Merbach, Inorg. Chem. 19 (1980) 3696.
[41] D.P. Riley, P.J. Lennon, W.L. Neumann, R.H. Weiss, J. Am. Chem. Soc. 119 (1997) 6522.
[42] (a) I. Ivanović-Burmazović, M.S.A. Hamza, R. van Eldik, Inorg. Chem. 41 (2002) 5150;
(b) I. Ivanović-Burmazović, M.S.A. Hamza, R. van Eldik, Inorg. Chem. 45 (2006) 1575.
[43] L. Batinic-Haberle, I. Spasojevic, P. Hambright, L. Benov, A.L. Crumbliss, I. Fridovich, Inorg. Chem. 38 (1999) 4011.
[44] N. Kasgai, T. Murase, T. Ohse, S. Nagaoka, H. Kawakami, S. Kubota, J. Inorg. Biochem. 91 (2002) 349.
[45] M. Momenteau, C.A. Reed, Chem. Rev. 94 (1994) 659.
[46] I. Schlichting, J. Berendzen, K. Chu, A.M. Stock, S.A. Maves, D.E. Benson, R.M. Sweet, D. Ringe, G.A. Petsko, S.G. Sligar, Science 287 (2000) 1615.
[47] K.P. Jensen, U. Ryde, J. Biol. Chem. 279 (2004) 14561.
[48] D.L. Wertz, J.S. Valentine, Struct. Bond. (Berl.) 97 (2000) 37.
[49] E. Kim, E.E. Chufan, K. Kamaraj, K.D. Karlin, Chem. Rev. 104 (2004) 1077.
[50] M. Selke, M.F. Sisemore, J.S. Valentine, J. Am. Chem. Soc. 118 (1996) 2008.
[51] M.F. Sisemore, M. Selke, J.N. Burstyn, J.S. Valentine, Inorg. Chem. 109 (1997) 979.
[52] E. McCandlish, A.R. Miksztal, M. Nappa, A.Q. Springer, J.S. Valentine, J.D. Strong, T.G. Spiro, J. Am. Chem. Soc. 102 (1980) 4268.
[53] J.N. Burstyn, J.A. Roe, A.R. Miksztal, B.A. Shaevitz, G. Lang, J.S. Valentine, J. Am. Chem. Soc. 110 (1988) 1382.
[54] K. Dürr, B.P. Macpherson, R. Warratz, F. Hempel, F. Tuczek, M. Helmreich, N. Jux, I. Ivanović-Burmazović, J. Am. Chem. Soc. 129 (2007) 4217.
[55] E.I. Solomon, U.M. Sundaram, T.E. Machonkin, Chem. Rev. 96 (1996) 2563.
[56] E.I. Solomon, P. Chen, M. Metz, S.-K. Lee, A.E. Palmer, Angew. Chem. Int. Ed. 40 (2001) 4570.
[57] E.A. Lewis, W.B. Tolman, Chem. Rev. 114 (2004) 1047.
[58] L.M. Mirica, X. Ottenwaelder, T.D.P. Stack, Chem. Rev. 114 (2004) 1013.
[59] L.Q. Hatcher, K.D. Karlin, J. Biol. Inorg. Chem. 9 (2004) 669.
[60] S. Schindler, Eur. J. Inorg. Chem. (2000) 2311.
[61] K.D. Karlin, S. Kaderli, A.D. Zuberbühler, Acc. Chem. Res. 30 (1997) 139.
[62] M. Becker, S. Schindler, K.D. Karlin, T.A. Kaden, S. Kaderli, T. Palanché, A.D. Zuberbühler, Inorg. Chem. 38 (1999) 1989.
[63] R. van Eldik, C.D. Hubbard, Adv. Phys. Org. Chem. 41 (2006) 1.
[64] M. Weitzer, M. Schatz, F. Hampel, F.W. Heinemann, S. Schindler, Dalton Trans. (2002) 686.
[65] J. Astner, M. Weitzer, S.P. Foxon, S. Schindler, F.W. Heinemann, J. Mukherjee, R. Gupta, V. Mahadevan, R. Mukherjee, Inorg. Chim. Acta 361 (2008) 279.
[66] T. Osaka, Y. Ueno, Y. Tachi, S. Itoh, Inorg. Chem. 42 (2003) 8087.
[67] S. Mahapatra, S. Kaderli, A. Llobert, T.-M. Neuhold, T. Palanché, J.A. Halfen, V.G. Young Jr., T.A. Kaden, L. Que Jr., A.D. Zuberbühler, W.B. Tolman, Inorg. Chem. 36 (1997) 6343.
[68] H.-C. Liang, C.X. Zhang, M.J. Henson, R.D. Sommer, K.R. Hatwell, S. Kaderli, A.D. Zuberbühler, E.I. Solomon, K.D. Karlin, J. Am. Chem. Soc. 124 (2002) 4170.
[69] M. Schatz, M. Becker, F. Thaler, F. Hampel, S. Schindler, R.R. Jacobson, Z. Tyeklar, N.N. Murthy, P. Ghosh, Q. Chen, J. Zubieta, K.D. Karlin, Inorg. Chem. 40 (2001) 2312.
[70] D. Utz, S. Kisslinger, F. Hampel, S. Schindler, J. Inorg. Biochem. 102 (2008) 1236.
[71] K.D. Karlin, N. Wei, B. Jung, S. Kaderli, P. Nicklaus, A.D. Zuberbühler, J. Am. Chem. Soc. 115 (1993) 9506.
[72] C.X. Zhang, S. Kaderli, M. Costas, E.-I. Kim, Y.-M. Neubold, K.D. Karlin, A.D. Zuberbühler, Inorg. Chem. 42 (2003) 1807.
[73] M. Becker, F.W. Heinemann, S. Schindler, Chem. Eur. J. 5 (1999) 3124.
[74] M. Schatz, M. Leibold, S.P. Foxon, M. Weitzer, F.W. Heinemann, F. Hampel, O. Walter, S. Schindler, Dalton Trans. (2003) 1480.
[75] A. Company, L. Gómez, R. Mas-Ballesté, I.V. Korendovych, X. Ribas, A. Poater, T. Parella, X. Fontrodona, J. Benet-Bucholz, M. Solà, L. Que Jr., E.V. Rybak-Akimova, M. Costas, Inorg. Chem. 46 (2007) 4997.
[76] (a) D. Maiti, D.-H. Lee, K. Gaoutchenova, C. Würtele, M.C. Holthausen, A.A. Narducci Sarjeant, J. Sundermeyer, S. Schindler, K.D. Karlin, Angew. Chem. Int. Ed. 47 (2008) 82;
(b) D. Maiti, J.S. Woetink, A.A. Naducci Sarjeant, E.I. Solomon, K.D. Karlin, Inorg. Chem. 47 (2008) 3787;
(c) S. Hong, L.M.R. Hill, A.K. Gupta, B.D. Naab, J.B. Gilroy, R.G. Hicks, C.J. Kramer, W.B. Tolman, Inorg. Chem. 48 (2009) 4514.
[77] E.I. Solomon, T.C. Brunold, M.I. Davis, J.H. Kemsley, S.-K. Lee, N. Lehnert, F. Neese, A.J. Skulan, Y.-S. Yang, J. Zhou, Chem. Rev. 100 (2000) 235.
[78] M. Costas, M.P. Mehn, M.P. Jensen, L. Que Jr., Chem. Rev. 104 (2004) 939.
[79] S.V. Kryatov, E.V. Rybak-Akimova, S. Schindler, Chem. Rev. 105 (2005) 2175.
[80] I.V. Korendovych, S.Y. Kryatov, E.V. Rybak-Akimova, Acc. Chem. Res. 40 (2007) 510.
[81] I.V. Korendovych, O.P. Kryatova, W.M. Rieff, E.V. Rybak-Akimova, Inorg. Chem. 46 (2007) 4197.
[82] (a) E. Reisner, T.C. Abikoff, S.J. Lippard, Inorg. Chem. 46 (2007) 10229;
(b) S. Yoon, S.J. Lippard, Inorg. Chem. 45 (2006) 4538;
(c) D. Lee, S.J. Lippard, Inorg. Chem. 41 (2002) 2704;
(d) J. Du Bois, T.J. Mizoguchi, S.J. Lippard, Coord. Chem. Rev. 200 (2000) 443;
(e) A.L. Feig, A. Masschein, A. Bakać, S.J. Lippard, J. Am. Chem. Soc. 119 (1997) 334;
(f) A.L. Feig, M. Becker, S. Schindler, R. van Eldik, S.J. Lippard, Inorg. Chem. 35 (1996) 2590;
(and references *loc cit*).
[83] S.V. Kryatov, F.A. Chavez, A.M. Reynolds, E.V. Rybak-Kryatov, L. Que Jr., W.B. Tolman, Inorg. Chem. 43 (2004) 2141.
[84] F.A. Chavez, R.Y.N. Ho, M. Pink, V.G. Young Jr., S.V. Kryatov, E.V. Rybak-Akimova, H. Andres, E. Munck, L. Que Jr., W.B. Tolman (Eds.), Angew. Chem. Int. 41 (2002) 149.
[85] M. Costas, C.W. Cady, S.V. Kryatov, M. Ray, M.J. Ryan, E.V. Rybak-Akimova, L. Que Jr., Inorg. Chem. 42 (2003) 7519.
[86] S.V. Kryatov, S. Taktak, I.V. Korendovych, E.V. Rybak-Akimova, J. Kaizer, S. Torelli, X. Shan, S. Mandal, V.L. MacMurdo, A. Mairata, I. Payeras, L. Que Jr., Inorg. Chem. 44 (2005) 85.
[87] X. Shan, L. Que Jr., Proc. Natl. Acad. Sci. U.S.A. 102 (2005) 5340.
[88] S.V. Kryatov, E.V. Rybak-Akimova, V.L. MacMurdo, L. Que Jr., Inorg. Chem 40 (2001) 2220.
[89] I.V. Korendovych, S.V. Kryatov, E.V. Rybak-Akimova, Acc. Chem. Res. 40 (2007) 510 (and references *loc cit*).
[90] A.E. Shilov, G.B. Shul'pin, Activation and catalytic reactions of saturated hydrocarbons in the presence of metal complexes, Kluwer Academic, Dordrecht, 2000.
[91] U. Fekl, K.I. Goldberg, Adv. Inorg. Chem. 54 (2003) 259.
[92] M. Lersch, M. Tilset, Chem. Rev. 105 (2005) 2471.
[93] B.J. Wik, M. Lersch, M. Tilset, J. Am. Chem. Soc. 124 (2002) 12116.
[94] M. Tilset, L. Johansson, M. Lersch, M. Tilset, ACS Symp. Ser. 885 (2004) 264.
[95] B.J. Wik, I. Ivanović-Burmazović, M. Tilset, R. van Eldik, Inorg. Chem. 45 (2006) 3613.
[96] J. Procelewska, A. Zahl, G. Liehr, R. van Eldik, N.A. Smyth, B.S. Williams, K.I. Goldberg, Inorg. Chem. 44 (2005) 7732.